AIAA SciTech Forum
8-12 January 2024, Orlando, FL
AIAA SCITECH 2024 Forum

10.2514/6.2024-2632

Validation of RANS-Based Round Jet Noise Models Using LES

Shabeeb N. P.* and Aniruddha Sinha†
Department of Aerospace Engineering, Indian Institute of Technology Bombay, Powai, Mumbai, 400076, INDIA

This paper re-evaluates the models of turbulent scales used in an existing modified Lilley's acoustic analogy for predicting the noise from round jets using steady Reynolds averaged Navier-Stokes solution fields. Such an investigation can only be pursued if one has reliable time-resolved flow data at hand. For this purpose, we use the LES database of an isothermal jet and a heated jet, both of which operate ideally-expanded at Mach 1.5 (Brès, G. A. et al., AIAA Journal, 55(4), 2017). The length and time scale models within the noise source model that take the mean turbulent kinetic energy and dissipation rate as inputs are in very good agreement with the direct calculations from the cross-correlation of the time-resolved LES data. The far-field spectra computed using the RANS-based scheme are in reasonable agreement with the reference spectra calculated directly from the time-resolved LES data using the Ffowcs Williams-Hawkings method. Additionally, we have proposed new model for the frequency-dependent length scale that is an ingredient of the overall noise model. Although the new model yields significant improvements in the jet near field, it results in only a minor improvement in the far-field spectra, specifically in the high frequencies at aft angles. Overall, the existing jet noise prediction tool is found to be robust.

I. Introduction

Jet noise is one of the most challenging fluid mechanics problems that researchers have been working on for the last few decades and it is also one of the loudest noises ever produced by mankind. The introduction of turbofan engines with progressively higher bypass ratios has successfully decreased jet noise by a significant margin. However, achieving further reductions in jet noise while maintaining other performance characteristics presents an immense challenge. Extensive research has focused on the development of quieter nozzle designs. This task is challenging due to cost constraints and the complex nature of the flow field. Gaining a comprehensive understanding of the flow field and identifying the sources of jet noise will serve as a guide for creating noise prediction tools and may ultimately lead to the realization of quieter designs.

Jet noise comprises three components: turbulent mixing noise, broadband shock-associated noise (BBSAN), and screech tones [1]. The latter two noise components occur exclusively in supersonic jets where imperfect expansion leads to the formation of a shock cell structure in the jet plume. In this paper, our focus is solely on turbulent mixing noise, which arises from the interaction between the jet and the surrounding ambient air, and is present in jets of all speeds. The approach to predicting jet noise encompasses several key elements. Specifically, a propagation operator and the corresponding noise source have to be identified, the latter have to be calculated or modelled, and the radiated sound has to be solved for. However, there is no clear separation between the source and the rest of the flow, nor a unique designation for the noise source. As a result, various options exist for reformulating the nonlinear flow equations into an acoustic analogy – an acoustic propagation equation forced by a corresponding sound source. The pioneering work of Lighthill [2] established the first theoretical formulation for aerodynamic noise prediction, where he reworked the Navier-Stokes equation (NSE) itself. Lighthill selected the free-space wave operator as the acoustic propagator, whence the source acquired a quadrupolar character. Lilley [3] subsequently modified Lighthill's equation to account for sound propagation through a medium with a locally-parallel shear, which is relevant for noise of shear flows and, specifically, jets. Later, Goldstein [4] proposed a generalized acoustic analogy that emerged as an exact consequence of the NSE, considering sound propagation through a medium with arbitrary shear. These progressive advancements aimed to shift the emphasis from modeling the noise source towards solving the acoustic wave operator.

Directly predicting the noise generated and radiated by turbulent flows using Direct Numerical Simulation (DNS) or Large Eddy Simulation (LES) is a computationally expensive and time-consuming task. In order to address this issue, Tam and Auriault [5] proposed a semi-empirical theory that enables the prediction of far-field noise from fine-scale

*Doctoral student
†Associate Professor, AIAA Member.

turbulence with minimal information required from a Computational Fluid Dynamics (CFD) database. This approach requires only the knowledge of the time-averaged (i.e., mean) fields of flow velocity, density, turbulent kinetic energy, and dissipation in the near-field region, thereby making the steady Reynolds-averaged Navier-Stokes (RANS) simulation a more economical and suitable choice for this purpose. The turbulent statistics in the source region are modeled using turbulent length scales, time scales, and velocity scales. The authors demonstrated the accuracy of their noise prediction model by comparing it to experimental measurements for single-stream round jets across a wide range of jet velocities and temperature ratios, particularly emphasizing the sideline and upstream directions where fine-scale contributions dominate. Building upon this work, Morris and Farassat [6] and Morris and Boluriaan [7] introduced an acoustic analogy based on the linearized Euler equations (LEE) without making assumptions about fine-scale or large-scale noise sources. This approach was also used by Raizada and Morris [8] for a Mach 0.9 jet, who presented comparisons with the noise results from the asymptotic solutions given by Balsa [9] and Goldstein [10]. Miller [11] presented an acoustic analogy that independently predicted the noise from turbulent mixing and shock interactions based on the LEE. Of late, this methodology has been successfully used to predict the noise from chevron jets and axisymmetric dual-stream jets for a wide range of Mach numbers and temperature ratios; it is employed in the present work too.

In all steady Reynolds averaged Navier-Stokes (RANS)-based noise prediction schemes, modeling the cross-correlation of the sources is necessary. These correlation models rely on local turbulent length scales, time scales, and velocity scales. The local turbulent length and time scales are estimated using simple scaling laws and empirical coefficients based on local $\overline{K} - \overline{\epsilon}$ data. Additionally, a frequency-dependent length scale model is employed to account for the contribution of different-sized eddies to far-field noise. The present study focuses on assessing the accuracy of these models by comparing them to the length and time scales computed directly from the cross-correlation of velocity fluctuations obtained from a well-validated Large Eddy Simulation (LES) database [12]. The LES database consists of two supersonic round jets – one isothermal and the other heated. Essentially, relevant time-averaged field quantities are extracted from the LES data and used as input for the RANS-based noise prediction model. The turbulent scales models within the noise source model that take the mean turbulent kinetic energy and dissipation rate as inputs are in very good agreement with the direct calculations from the cross-correlation of the time-resolved LES data. The far-field sound predicted using the RANS-based scheme closely matches the sound directly propagated from time-resolved LES data using the Ffowcs Williams-Hawkings (FW-H) approach. In the process, we propose an improved model for the frequency-dependent length scales of the flow, which appears to perform better than the existing model for the same.

II. Predicting jet noise from RANS

Our mathematical formulation of the jet noise prediction model is based on the works of Refs. [5–8, 11].

A. The forced acoustic wave equation

The governing equations are the Euler equations as viscous effects are deemed unimportant for both sound generation and propagation. The equations are

$$\frac{D\pi}{Dt} + \boldsymbol{\nabla}\cdot\boldsymbol{u} = 0, \qquad \frac{D\boldsymbol{u}}{Dt} + a^2\boldsymbol{\nabla}\pi = 0. \tag{1}$$

where $D(\cdot)/Dt$ is the material derivative, a is the local speed of sound and $\pi := (1/\gamma)\ln(p/p_\infty)$ is the logarithmic pressure. The Euler equations are linearized by expanding the flow variables as fluctuations (indicated by a prime) on a time-averaged base state (indicated by an overline). Introducing the base flow material derivative $\overline{D}(\cdot)\Big/\overline{D}t := \partial(\cdot)/\partial t + \overline{\boldsymbol{u}}\cdot\boldsymbol{\nabla}(\cdot)$, these equations are re-written as

$$\frac{\overline{D}\pi'}{\overline{D}t} + \boldsymbol{\nabla}\cdot\boldsymbol{u}' = -\boldsymbol{u}'\cdot\boldsymbol{\nabla}\pi' =: f_0, \qquad \frac{\overline{D}\boldsymbol{u}'}{\overline{D}t} + \boldsymbol{u}'\cdot\boldsymbol{\nabla}\overline{\boldsymbol{u}} + \overline{a^2}\boldsymbol{\nabla}\pi' = -\boldsymbol{u}'\cdot\boldsymbol{\nabla}\boldsymbol{u}' - \left(a^2\right)'\boldsymbol{\nabla}\pi' =: \boldsymbol{f}. \tag{2}$$

The nonlinear terms on the RHS constitute noise sources. The linearized Euler equations (LEE) may be solved by convolving its vector Green's function with the source.

Considering a locally parallel mean flow for a round jet, the LEE has been simplified to the Lilley's equation [3]. The equations are expressed in cylindrical coordinates (x, r, ϕ) to facilitate modelling of the axisymmetric jets that are of interest here. The Lilley's operator acting on the logarithmic pressure component of vector Green's function of the

LEE ($\widehat{\pi}_g^n$) in the temporal Fourier domain can then be written as

$$\left(\overline{D}_\omega^3 - \overline{a^2}\,\overline{D}_\omega\nabla^2 - \frac{d\overline{a^2}}{dr}\overline{D}_\omega\frac{\partial}{\partial r} + 2\overline{a^2}\frac{d\overline{u}}{dr}\frac{\partial^2}{\partial x\partial r}\right)\widehat{\pi}_g^n(\boldsymbol{x}|\boldsymbol{x}_s;\omega) = \overline{D}_\omega^2\left(\delta(\boldsymbol{x}-\boldsymbol{x}_s)\right)\delta_{0n} - \overline{D}_\omega\frac{\partial}{\partial x}\delta(\boldsymbol{x}-\boldsymbol{x}_s)\,\delta_{xn}$$
$$-\left[\frac{1}{r}\overline{D}_\omega\frac{\partial}{\partial r}\left(r\delta(\boldsymbol{x}-\boldsymbol{x}_s)\right) - 2\frac{d\overline{u}}{dr}\frac{\partial}{\partial x}\delta(\boldsymbol{x}-\boldsymbol{x}_s)\right]\delta_{rn} - \frac{1}{r}\overline{D}_\omega\frac{\partial}{\partial\phi}\delta(\boldsymbol{x}-\boldsymbol{x}_s)\,\delta_{\phi n} =: \mathscr{S}^n(\boldsymbol{x}-\boldsymbol{x}_s;\omega), \tag{3}$$

where the operator on the LHS is Lilley's wave operator, $\overline{u}$ is the mean velocity component in the streamwise (i.e., x) direction, and $\overline{D}_\omega := -i\omega + \overline{u}\partial/\partial x$. The vector Green's functions are indexed by n, which takes values in $\mathscr{N} := \{0, x, r, \phi\}$ corresponding to forcing of the conservation equations for mass and three cylindrical components of momentum (see eqn. (2)).

Let the scalar Green's function of the above Lilley's equation be denoted as $\widehat{g}(\boldsymbol{x}|\boldsymbol{x}_s;\omega)$. Then the pressure component of the vector Green's function of LEE can be written as the convolution integral

$$\widehat{\pi}_g^n(\boldsymbol{x}|\boldsymbol{x}_s;\omega) = \iiint \widehat{g}(\boldsymbol{x}|\boldsymbol{x}_t;\omega)\,\mathscr{S}^n(\boldsymbol{x}_t-\boldsymbol{x}_s;\omega)d\boldsymbol{x}_t. \tag{4}$$

The Green's function of the Lilley's equations are solved numerically using the adjoint approach, as explained by Tam and Auriault [13] and Raizada and Morris [8]; subsequently, the pressure component of the vector Green's functions of LEE are determined using eqn. (4). The far-field pressure fluctuations may be obtained by convolving the four Green's functions' pressure components with the corresponding sources of the LEE.

B. Modelling of sources

Since we are invariably interested only in the spectral density of the pressure (and not its time history), only the spatio-temporal cross-correlations of the source terms have to be modelled [11]. Based on extensive round jet databases accumulated over decades, such a model has been proposed by many researchers [5, 7, 14], and is of the form

$$\langle f_n(\boldsymbol{x},t)f_{n'}(\boldsymbol{x}+\boldsymbol{\eta},t+\tau)\rangle_t = \delta_{nn'}A_n(\boldsymbol{x})\exp\left\{-\frac{|\tau|}{\tau_s(\boldsymbol{x})} - \frac{(\eta_x-\overline{u}(\boldsymbol{x})\tau)^2}{\ell_x^2(\boldsymbol{x})} - \frac{\eta_y^2}{\ell_y^2(\boldsymbol{x})} - \frac{\eta_z^2}{\ell_z^2(\boldsymbol{x})}\right\}, \quad n\in\{x,r,\phi\}. \tag{5}$$

Here, for convenience of modelling, we have switched to Cartesian coordinates, such that the spatial separation vector is $\boldsymbol{\eta} = \eta_x\hat{\boldsymbol{i}} + \eta_y\hat{\boldsymbol{j}} + \eta_z\hat{\boldsymbol{k}}$. At zero-time lag, this ansatz posits a Gaussian decay of the two-point cross-correlation in all three Cartesian coordinate directions, albeit with different length scales ℓ_x, ℓ_y, ℓ_z. Moreover, it invokes the frozen field hypothesis and models an exponential decay of correlation with time, having time scale τ_s, if one were to move with the mean flow (assumed negligible in the cross-stream directions for this purpose). Further, it is assumed that each source term is correlated only with itself and is uncorrelated with all other source terms. Finally, the model assumes the behavior of the correlation terms to be the same for all the sources, albeit with different amplitudes that are related by dimensional analysis to the local velocity scale u_s and the above length and time scales as

$$A_0(\boldsymbol{x}) = B_0^2\frac{(u_s(\boldsymbol{x})/a_\infty)^4}{\tau_s^2(\boldsymbol{x})}, \qquad A_n(\boldsymbol{x}) = B_{>0}^2\frac{(u_s(\boldsymbol{x})/a_\infty)^2u_s^4(\boldsymbol{x})}{\ell_x^2(\boldsymbol{x})}, \quad n\in\{x,r,\phi\}. \tag{6}$$

Here, B_0 and $B_{>0}$ are empirical constants.

In a steady RANS-based noise prediction model, the local length, time and velocity scales are determined from the local mean turbulent kinetic energy $\overline{K}(\boldsymbol{x})$ and dissipation $\overline{\epsilon}(\boldsymbol{x})$ using simple scaling laws [5–8, 11]:

$$u_s(\boldsymbol{x}) = c_u\sqrt{\frac{2}{3}\overline{K}(\boldsymbol{x})}, \qquad \tau_s(\boldsymbol{x}) = c_\tau\frac{\overline{K}(\boldsymbol{x})}{\overline{\epsilon}(\boldsymbol{x})}, \qquad \ell_x(\boldsymbol{x}) = c_\ell\frac{\{\overline{K}(\boldsymbol{x})\}^{3/2}}{\overline{\epsilon}(\boldsymbol{x})}, \qquad \ell_y(\boldsymbol{x}) = \ell_z(\boldsymbol{x}) = \frac{\ell_x(\boldsymbol{x})}{3}. \tag{7}$$

where, c_ℓ, c_τ and c_u are empirical constants. Note that the cross-stream length scales are invariably assumed to be one-third their streamwise counterpart.

Subsequently, we would need to model the source cross-correlations presented in eqn. (5) in the frequency domain. Although all the other scales carry over from their time-averaged counterparts modelled above, the turbulent length scales can be expected to depend on the frequency. Corresponding to the radial frequency ω, the Strouhal number is defined as

LES Case	M_j	T_j/T_∞	M_a	Re_j
B118	1.5	1.0	1.5	300,000
B122	1.5	1.74	1.98	155,000

Table 1 **Test cases used from LES database of Ref. [12].**

$St = \omega D_j/(2\pi U_j)$, where D_j is the jet's nozzle-exit diameter, and U_j is its nozzle-exit velocity. Morris and Zaman [15] modelled the frequency-dependent length scales (note the subtle change in notation from the frequency-independent variants) as

$$l_i(\boldsymbol{x},\omega) = \ell_i(\boldsymbol{x})\frac{1-\mathrm{e}^{-c_f St}}{c_f St}, \quad \forall i \in \{x,y,z\}. \tag{8}$$

The empirical constant $c_f = 11.25$ was chosen to match the experimental observations [15]. Subsequently, we propose an improvement to this model based on the LES data at hand.

C. The far-field spectrum

Without loss of generality, the spherical coordinates of an observer can be expressed as $\boldsymbol{x} := (R, \Theta, \phi = 0)$, owing to the axisymmetry of the jets being considered in this work. Here, R is the polar radius of the observer (i.e., the distance from the jet nozzle exit's center), Θ is the polar angle of the observer measured with respect to the jet downstream axis, and the observer is assumed to be at $z = 0$ such that its azimuthal angle is zero. Then, assuming that the observer is in the far field, and that the vector Green's function of two closely-placed source points differ only by a phase factor [5], the relevant spectral density of pressure fluctuations can be approximated as

$$\begin{aligned} S_p(\boldsymbol{x},\omega) &= 2\pi^{3/2}(\gamma p_\infty)^2 \sum_{n\in\mathcal{N}} \iiint \left|\widehat{\pi}_g^n(\boldsymbol{x}\,|\boldsymbol{x}_s;\omega)\right|^2 \sigma_n(\boldsymbol{x}_s;\boldsymbol{x},\omega)\,d\boldsymbol{x}_s, \\ \sigma_n(\boldsymbol{x}_s;\boldsymbol{x},\omega) &:= A_n(\boldsymbol{x}_s)\frac{l_x^3(\boldsymbol{x}_s;\omega)}{9}\tau_s(\boldsymbol{x}_s)\frac{\exp\left\{-\omega^2(1+8\cos^2\Theta)l_x^2(\boldsymbol{x}_s;\omega)/(36a_\infty^2)\right\}}{1+\omega^2\tau_s^2(\boldsymbol{x}_s)(1-\overline{u}(\boldsymbol{x}_s)\cos\Theta/a_\infty)^2}. \end{aligned} \tag{9}$$

In the above, the frequency-dependent length scales are introduced, and the relation between the cross-stream and streamwise length scales presented in eqn. (7) is used implicitly.

III. Results and discussion

To predict far-field jet noise using the model described in the previous sections, a steady Reynolds averaged Navier-Stokes (RANS) solution is sufficient. However, if we aim to *validate* such a model, independent noise predictions are required, which cannot be obtained from the RANS data. Instead, the Large Eddy Simulation (LES) results from Brès et al. [12] are employed, and the necessary input parameters are computed based on this data. The database consists of two cases: an isothermal ideally-expanded round jet (case B118) and a heated ideally-expanded round jet (case B122), summarized in Table 1. The mid-field and far-field sound were predicted from the LES using the FW-H approach [16], and these were found to be in very good agreement with counterpart experiments [17]. The LES grid used was unstructured and had 42 million control volumes; for the current analysis, this data was down-sampled onto a cylindrical structured grid containing approximately 1.3 million points. Specifically, the streamwise extent was limited to $20D_j$.

To calculate the Green's function, the mean streamwise velocity $\overline{u}$ and density $\overline{\rho}$ are required; these are presented in fig. 1 for both the jets. The mean density field of the isothermal B118 jet is essentially uniform, and is hence omitted. Note that the spatial coordinates (viz. x and r) are implicitly normalized by D_j here and subsequently. To obtain the radial derivatives robustly, each radial profile of $\overline{u}$ is fitted with a truncated Gaussian function [18], and the fit parameters are then smoothed using cubic splines [19]. As depicted in the same figure, the fitted-and-smoothed result matches well with the original data. A similar smoothing procedure is applied to the mean density field. Using these $\overline{u}$ and $\overline{\rho}$ as input, the vector Green's functions of the LEE are computed for both the jets; the program is written in MATLAB following the theory laid out in the preceding section as well as in the references cited therein.

For later reference, fig. 2 presents the time-averaged normalized turbulent kinetic energy calculated in the two jet databases. As expected, the turbulent kinetic energy is non-trivial only in the jet shear layer.

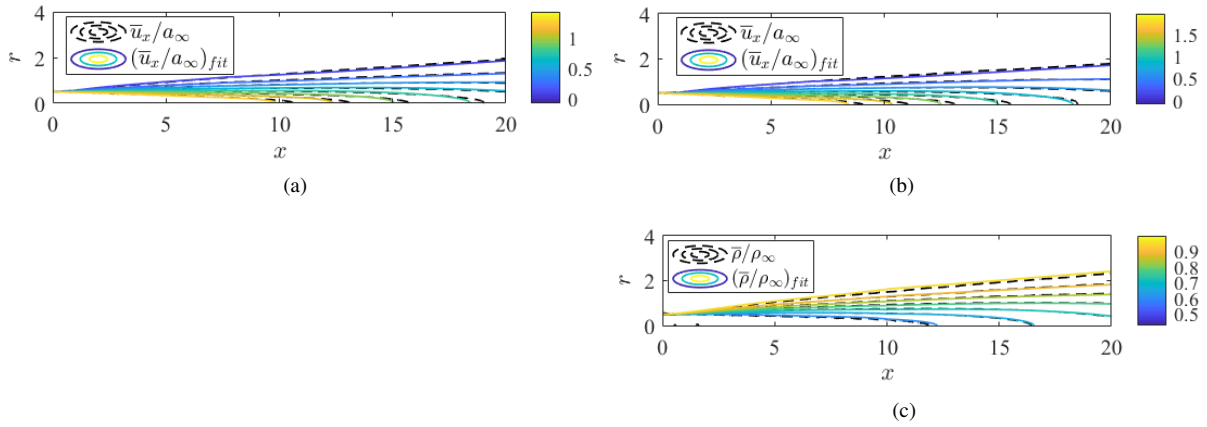

Fig. 1 **The mean streamwise velocity fields of (a) the B118 and (b) the B122 jets, and (c) the mean density field of the B122 jet. Comparisons are presented of the raw fields with their fitted-and-smoothed counterparts.**

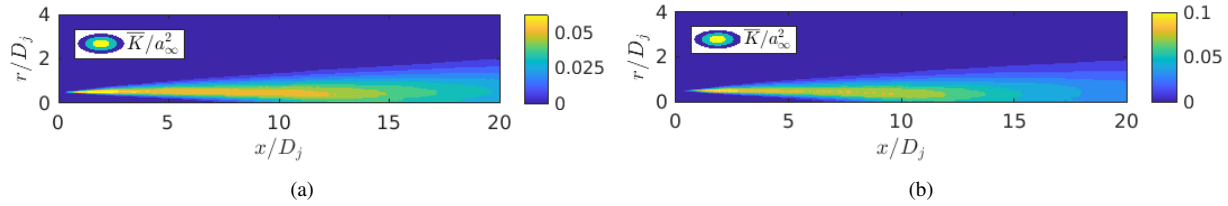

Fig. 2 **Contours of mean values of normalized turbulent kinetic energy of (a) B118 and (b) B122 jets.**

A. Validating the time and frequency-independent length scale models

We evaluate two alternate approaches of obtaining the necessary inputs to the noise prediction technique – i.e., the length, time and velocity scales. In the first approach, we estimate the frequency-independent length scale and time scale from the LES data directly using suitable cross-correlations of the fluctuating streamwise velocity field timeseries. In the second approach, we calculate the mean turbulent kinetic energy and dissipation from the LES data, and then find these scales from the models presented in eqn. (7). The velocity scale is obtained from the TKE in the manner outlined in eqn. (7) in both approaches. Moreover, in this initial assessment, we continue to use the existing approach for arriving at the frequency-dependent length scales l_i from the frequency-independent ones ℓ_i, as outlined in eqn. (8); an improvement is described in Section III.C.

For the first approach, we should be looking at the correlations of the forcing functions f_0 and $\boldsymbol{f}$ (see eqns. (2) and (5)). However, given the generality of the source model in eqn. (5) that assumes the same scales to apply to all the forcing function components, as well as the dependence of the forcing functions on the primitive flow variables, we analyze the streamwise velocity fluctuations u' instead. Figure 3 presents the spatio-temporal cross-correlation of u' at $x = 5D_j$, $r = 0.5D_j$ for the B118 jet. It is observed that the correlation curve for any given streamwise separation η_x resembles a Gaussian, with the peak shifting to a time lag τ that is in almost exact accordance with $\eta_x/\overline{u}$. Moreover, the maximum correlation coefficient decays almost exponentially with η_x. Together, these substantiate the validity of the Gaussian-exponential ansatz of eqn. (5).

The local time scale $\tau_s(\boldsymbol{x})$ is determined by fitting with an exponential the peaks of the local two-point two-time cross-correlation data (i.e., $\eta_y = 0$ and $\eta_z = 0$, and $\eta_x = \overline{u}\tau$). The local (frequency-independent) streamwise length scale $\ell_x(\boldsymbol{x})$ is determined by fitting with a Gaussian the local cross-correlation data at finite streamwise separation and no separation in other coordinates (i.e., $\tau = 0$, $\eta_y = \eta_z = 0$).

The length and time scales computed from the cross-correlation data are presented in figs. 4(a) and 4(b) respectively for the heated B122 jet. The reliable estimation of the time scale becomes especially difficult outside the shear layer because of decay of correlation; thus, the values are hard set to zero thereat. This is not an issue for the implementation since eqn. (6) shows that the noise source itself vanishes in regions where the velocity scale (and so the TKE) vanishes, which happens outside the shear layer. The shear layer starts out being very thin near the nozzle exit and thickens as one

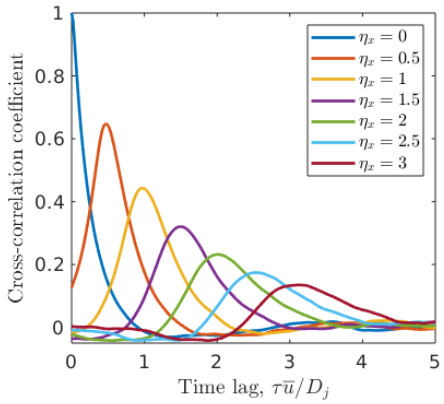

Fig. 3 **Variation of cross-correlation coefficient with the time lag at various axial spatial lag at $r = 0.5D_j$, $x = 5D_j$ (B118 jet).**

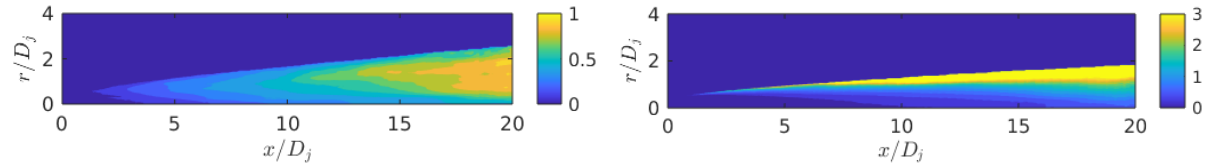

Fig. 4 **(a) Normalized frequency-independent streamwise length scale ℓ_x/D_j and (b) normalized time scale $\tau_s a_\infty/D_j$, computed for the B122 jet using u' cross-correlation data.**

moves downstream. As expected, the turbulent length scale increases downstream as the shear layer thickens, reflecting a corresponding enlarging of turbulent structures. Since larger structures have greater temporal persistence, the time scales also increase as one goes downstream, and especially near the outer edge of the shear layer.

In the second approach, the local turbulent scales are found from the model of eqn. (7) using the mean TKE and dissipation rate of the LES database. The evaluation of the mean turbulent dissipation rate $\overline{\epsilon}$ from LES data is not obvious, especially when the data is downsampled in space as is the case here. We follow a Smagorinsky-type closure model approach [20] that gives the following estimate in Cartesian tensor notation:

$$\overline{\epsilon} = (C_s\Delta)^2 \left\langle \frac{1}{2}\left(\frac{\partial u_i'}{\partial x_j} + \frac{\partial u_j'}{\partial x_i}\right)^2 \right\rangle^{3/2}.$$

Here, $< \cdot >$ stands for averaging in time, C_s is the Smagorinsky constant whose typical value may be taken as 0.17 [21], and Δ is the grid scale. Converting this to cylindrical coordinates with streamwise, radial and azimuthal velocity components as u, v and w respectively, we have

$$\begin{aligned}\overline{\epsilon} = (C_s\Delta)^2 \Bigg\langle & 2\left(\frac{\partial v'}{\partial r}\right)^2 + \left(\frac{\partial w'}{\partial r}\right)^2 + \left(\frac{\partial u'}{\partial r}\right)^2 + \left(\frac{1}{r}\frac{\partial v'}{\partial \phi} - \frac{w'}{r}\right)^2 + 2\left(\frac{1}{r}\frac{\partial w'}{\partial \phi} + \frac{v'}{r}\right)^2 + \left(\frac{1}{r}\frac{\partial u'}{\partial \phi}\right)^2 \\ & + \left(\frac{\partial v'}{\partial x}\right)^2 + \left(\frac{\partial w'}{\partial x}\right)^2 + 2\left(\frac{\partial u'}{\partial x}\right)^2 + 2\left(\frac{1}{r}\frac{\partial v'}{\partial \phi} - \frac{w'}{r}\right)\frac{\partial w'}{\partial r} + 2\frac{\partial u'}{\partial r}\frac{\partial v'}{\partial x} + 2\frac{1}{r}\frac{\partial u'}{\partial \phi}\frac{\partial w'}{\partial x}\Bigg\rangle^{3/2}. \end{aligned} \tag{10}$$

Invoking the statistical axisymmetry of the jets investigated here, the $< \cdot >$ operator is now be taken to denote averaging in time and azimuth.

We will be estimating ϵ at the lipline (i.e., $r = D_j/2$) to assess the validity of the existing models for the length and time scales based on $\overline{K}$ and $\overline{\epsilon}$. In the structured cylindrical grid used for downsampling the LES data, the radial grid is non-uniform with a resolution $0.01D_j$ at the lipline. The streamwise grid spacing is $0.0625D_j$, and the azimuthal

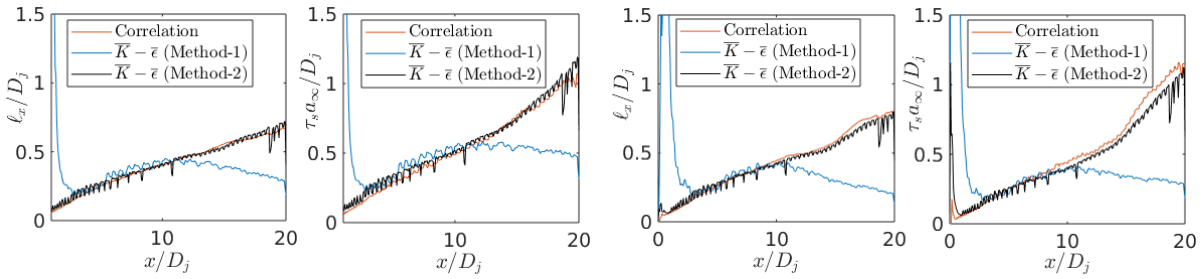

Fig. 5 **Normalized frequency-independent streamwise length scale ℓ_x/D_j and normalized time scale $\tau_s a_\infty/D_j$ computed for (a) B118 and (a) B122 jet along the lipline.**

grid spacing is $\pi/12$ radians. At the lipline, the latter results in a circumferential grid spacing of $\pi D_j/24 = 0.13D_j$. Our first method of estimating the dissipation rate downsamples the streamwise and radial grids to match this coarsest circumferential grid, so that the consistent grid spacing becomes $\Delta = 0.13D_j$.

However, a better approach may be to use the available grid resolution in each direction to estimate the respective gradients. For this, we modify the above equation to

$$\begin{aligned}\overline{\epsilon} = C_s^2\Bigg\langle &\Delta_r^{4/3}\left\{2\left(\frac{\partial v'}{\partial r}\right)^2+\left(\frac{\partial w'}{\partial r}\right)^2+\left(\frac{\partial u'}{\partial r}\right)^2\right\}+\Delta_\phi^{4/3}\left\{\left(\frac{1}{r}\frac{\partial v'}{\partial \phi}-\frac{w'}{r}\right)^2+2\left(\frac{1}{r}\frac{\partial w'}{\partial \phi}+\frac{v'}{r}\right)^2+\left(\frac{1}{r}\frac{\partial u'}{\partial \phi}\right)^2\right\}\\ &+\Delta_x^{4/3}\left\{\left(\frac{\partial v'}{\partial x}\right)^2+\left(\frac{\partial w'}{\partial x}\right)^2+2\left(\frac{\partial u'}{\partial x}\right)^2\right\}\\ &+2(\Delta_\phi\Delta_r)^{2/3}\left(\frac{1}{r}\frac{\partial v'}{\partial \phi}-\frac{w'}{r}\right)\frac{\partial w'}{\partial r}+2(\Delta_x\Delta_r)^{2/3}\frac{\partial u'}{\partial r}\frac{\partial v'}{\partial x}+2(\Delta_\phi\Delta_x)^{2/3}\frac{1}{r}\frac{\partial u'}{\partial \phi}\frac{\partial w'}{\partial x}\Bigg\rangle^{3/2}. \end{aligned} \tag{11}$$

Here, the grid scales in the three coordinate directions at the jet lipline are $\Delta_x = 0.0625D_j$, $\Delta_r = 0.01D_j$ and $\Delta_\phi = 0.13D_j$.

The length scales and time scales obtained using the $\overline{K}-\overline{\epsilon}$ data are presented in fig. 5 along with the correlation data. For this, the tuning parameters are c_ℓ and c_τ, which we discuss subsequently. We have used two methods for the computation of the dissipation rate as discussed above. The length scales and time scales computed using the constant grid scale $\Delta = 0.13D_j$ (eqn. (10)) is labelled '$\overline{K}-\overline{\epsilon}$ (Method-1)' in fig. 5. The turbulent scales computed using the different grid scales in radial, azimuthal and streamwise directions (eqn. (11)) is labelled '$\overline{K}-\overline{\epsilon}$ (Method-2)' in fig. 5. The results obtained using 'Method-2' almost perfectly match the turbulent scales derived from the correlation. To obtain the match seen in these figures, the tuning parameters were chosen as

$$c_\ell = 0.35, \quad c_\tau = 0.09. \tag{12}$$

The turbulent scales obtained using 'Method-1' also match with the correlation and 'Method-2' results, but only over a limited streamwise extent (viz. $x/D_j \in [2, 10]$). Near the nozzle, the large radial grid spacing misses the thin shear layer completely, thereby resulting in a large under-estimation of $\overline{\epsilon}$, in turn leading to the significant over-prediction of the length and time scales observed. On the other hand, the errors incurred downstream of $x = 10D_j$ by 'Method-1' are possibly due to the over-estimation of radial gradients in the shear layer by the coarser grid. Overall, we find that the proposed non-isotropic grid estimate of $\overline{\epsilon}$ in eqn. (11) is the better approach compared to the isotropic grid estimate of eqn. (10). More importantly, we confirm that the two approaches for the computation of turbulent scales – directly from correlations of u' and from the $\overline{K}-\overline{\epsilon}$ model of eqn. (7) – yield quantitatively similar results along the lipline of both the isothermal and heated supersonic jets, thereby serving to validate the latter. Note that the best-fit scale constants c_ℓ and c_τ found here in eqn. (12) are quite close to those reported in the recent literature [11] (viz. 0.4 and 0.06, respectively).

We did not calculate the dissipation rate in the entire jet. So, we will proceed with far-field noise predictions from the correlation-based ℓ_x and τ_s fields. With the frequency-independent length scale in hand, the frequency-dependent length scales are estimated using the existing model of eqn. (8). The parameter c_f appearing in this model is set to

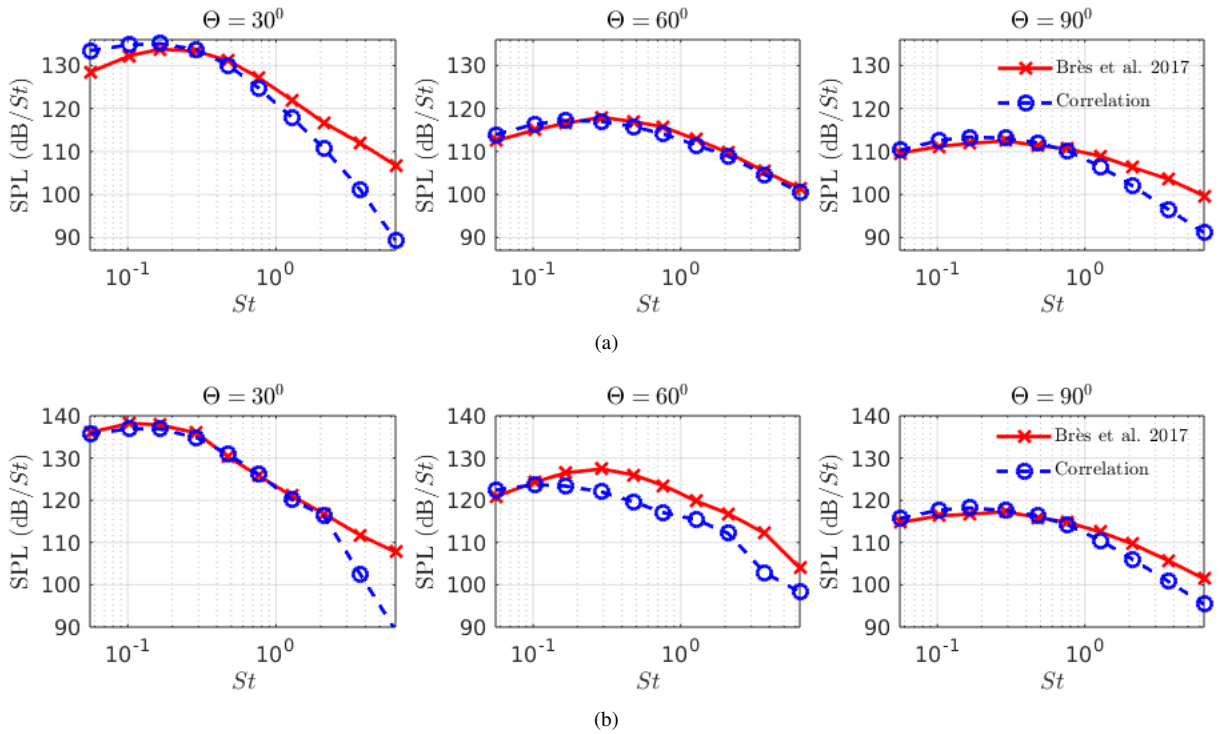

Fig. 6 **Far-field noise spectra predicted using turbulent scales ℓ_x and τ_s derived from correlation data compared with corresponding FW-H calculations reported by Brès et al. [12] for (a) the B118 and (b) the B122 jets.**

11.25 as mentioned in its discussion earlier. Another parameter is the velocity scale coefficient c_u seen in eqn. (7), which is set as $c_u = 1.0$ following the literature [11]. The only remaining free parameters are the amplitude coefficients B_0 and $B_{>0}$ appearing in eqn. (6), which are found from a fit with the far-field spectra as described below.

The far-field noise spectra (in terms of sound pressure level, SPL) are calculated using the turbulent scales obtained from the correlation data at three representative polar angles using eqn. (9), and presented in fig. 6. The polar radii of these observer positions are chosen to match the location of microphones in the reference experiments [17], wherein a rectilinear array was used. In particular, the polar radii of the 30°, 60° and 90° microphones are $66.4D_j$, $69.3D_j$ and $60D_j$, respectively. The reference noise spectra are taken from the original paper [12] reporting the LES database, where it was calculated from the time-resolved fluctuating flow field using the FW-H method. The authors reported an excellent match with the counterpart experimental data [17], which validated the LES simulations.

The comparison of our far-field spectral predictions with the reference is quite reasonable, except at high frequencies. It is evident that the severely approximate model performs very satisfactorily vis-à-vis the much more input-heavy reference approach. To obtain these spectral agreement, we consistently set the amplitude parameters as:

$$B_0 = 0.008, \quad B_{>0} = 5.446. \tag{13}$$

That is, these values were used across both the jets, and definitely in calculations across all observer locations for a particular jet. These values are obtained by minimizing the error between the reference spectra and the ones predicted from the turbulent scales derived from the correlation data, across all frequencies and observer locations for both the jets.

In summary, we show that the correlation-based approach yields length and time scales along the jets' lipline that are in good agreement with their models based on $\overline{K}$ and $\overline{\epsilon}$. Then, the correlation-based method's far-field spectral match presented here serves to validate the noise prediction model based on RANS solutions in an indirect manner.

B. Validating the frequency-dependent length scale model

In this section, we probe the validity of the existing frequency-dependent length scale model originally proposed by Morris and Zaman [15], subsequently employed by Miller [11], and presented here in eqn. (8). Consistent with the

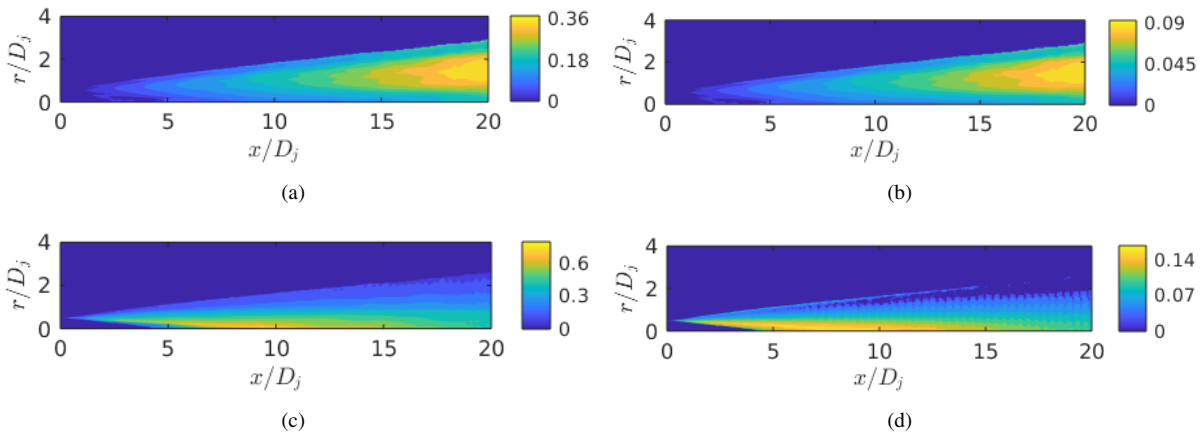

Fig. 7 **Normalized frequency-dependent streamwise length scale l_x/D_j in the B118 jet calculated from (a), (b) the existing model of eqn. (8) and (c), (d) the cross-coherence data, at (a), (c) $St = 0.2$ and (b), (d) $St = 0.9$.**

spatio-temporal correlation approach adopted in the previous section for calculating the frequency-independent length scale from the LES database, we now look at the two-point *coherence* of the streamwise velocity fluctuations u'.

We start by dividing the time data of u' into J segments with 50% overlap. Temporal Fourier transform is applied to each data segment, with a Hanning window function applied to minimize boundary discontinuities. Let us denote the resulting frequency-domain velocity field for the j^{th} segment by $\widehat{u}^{(j)}(\boldsymbol{x};\omega)$, where $\boldsymbol{x}$ is the position of the virtual probe and ω is the circular frequency. The corresponding cross-coherence with a positional separation vector of $\boldsymbol{\eta}$ is then calculated as

$$C_{uu}(\boldsymbol{\eta};\boldsymbol{x},\omega) = \frac{J^{-1}\sum_{j=1}^{J}\left[\widehat{u}^{(j)}(\boldsymbol{x};\omega)\left\{\widehat{u}^{(j)}(\boldsymbol{x}+\boldsymbol{\eta};\omega)\right\}^{*}\right]}{\sqrt{J^{-1}\sum_{j=1}^{J}\left|\widehat{u}^{(j)}(\boldsymbol{x};\omega)\right|^2}\sqrt{J^{-1}\sum_{j=1}^{J}\left|\widehat{u}^{(j)}(\boldsymbol{x}+\boldsymbol{\eta};\omega)\right|^2}}. \tag{14}$$

(This approach for estimating the coherence follows from the well-known Welch spectrogram methodology.) Finally, following eqn. (5), we fit a Gaussian function of the form $\exp\{-(\eta_x/l_x)^2\}$ for $\boldsymbol{\eta} = \eta_x\hat{\boldsymbol{\imath}}$ (i.e., a separation in the axial direction alone) to the *real part* of the cross-coherence function in order to estimate the corresponding frequency-dependent streamwise length scale $l_x(\boldsymbol{x},\omega)$.

Figure 7 presents the frequency-dependent length scale in the B118 jet calculated from the above coherence approach at two representative frequencies. A comparison is made with the corresponding scales obtained by applying the model of eqn. (8) to the frequency-independent length scale found from the correlation data, with the coefficient c_f set to 11.25 as before. No similarity exists between the results from the two approaches! Considering the $St = 0.2$ case, the model predicts the largest scales towards the downstream end of the domain near the middle of the shear layer. On the other hand, the coherence data yields the largest scales just after the end of the potential core near the inner edge of the shear layer. The model necessarily results in a wholesale scaling down of the length scale as one goes to higher frequencies, without affecting the distribution in any way. Although the coherence data does not result in the same length scale distribution by any means, it also displays a similar wholesale scaling down of the length scale with increasing frequency. This gives some hope that the existing model may be tweaked to improve it, rather than be discarded entirely.

C. A new model for the frequency-dependent length scale

An improved frequency-dependent length scale model may be arrived at by a deeper investigation of the coherence result. For this, fig. 8 studies the length scale distribution with frequency at several streamwise locations along the lipline (i.e., $r = 0.5D_j$) for both the jets. One observes a monotonic decay with frequency in all cases, which again supports the essential validity of the existing model of eqn. (8). The predictions from this model (using the frequency-*independent* length scale ℓ_x found from the correlation data) are overlaid on the coherence results. One observes an identical qualitative trend, although severe discrepancies exist in the values in all but the most downstream station. As a guide to

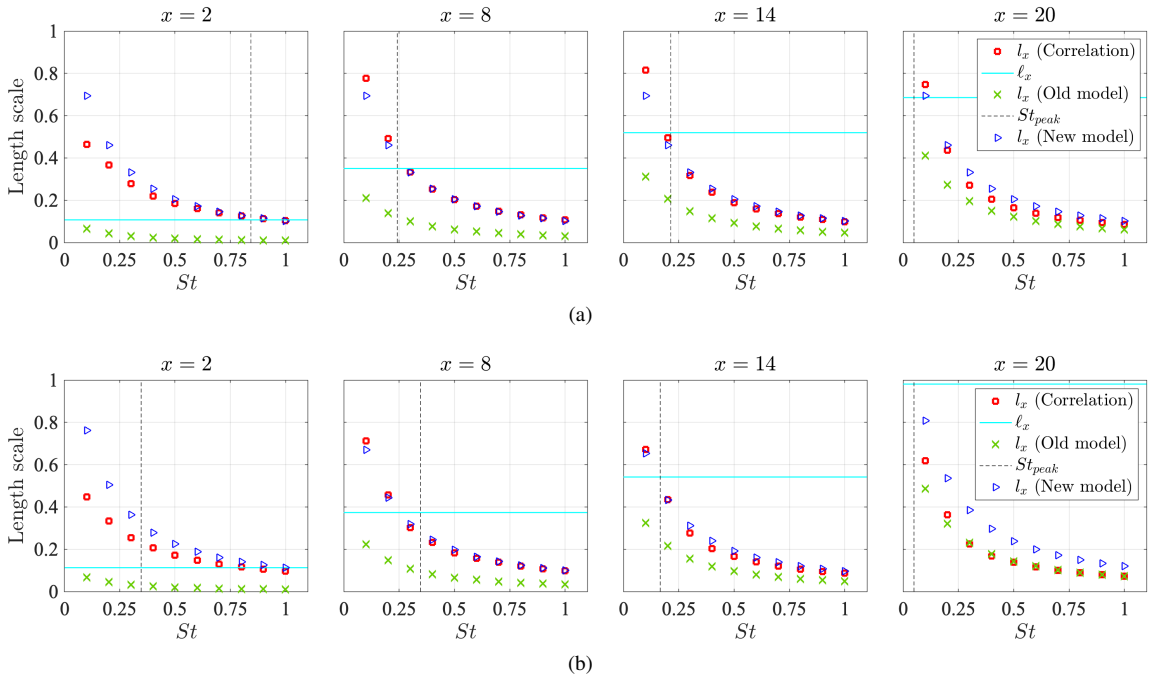

Fig. 8 **Variation of the frequency-dependent streamwise length scale l_x computed from the cross-coherence of streamwise velocity fluctuations, presented at four streamwise locations along the lipline for (a) the B118, and (b) the B122 jets. These are compared with the predictions from the existing (i.e., 'old') and the proposed (i.e., 'new') models, both using the local frequency-independent streamwise length scales ℓ_x (also shown) obtained from the correlation data. The respective peak frequencies identified from pressure spectra are also indicated.**

understanding this, the ℓ_x is indicated in each plot; the model of course results in the frequency-dependent length scale l_x equalling ℓ_x at $St = 0$.

A perusal of fig. 8 suggests that an improved l_x model may be obtained if it has the existing decay with St, but matches the local ℓ_x at successively lower frequencies with increasing downstream distance. This is not entirely surprising. As one progresses downstream along the jet plume, the dominant length scale shifts to lower frequencies indeed, due to the growth of the coherent structures in the thickening shear layer. This should most naturally cause $l_x(\boldsymbol{x}, St^*) = \ell_x(\boldsymbol{x})$ to occur at lower Strouhal numbers St^* for increasing x. An estimate of $St^*(\boldsymbol{x})$ may be sought in the peak frequency of the local spectrum. For consistency, one should look at the spectrum of streamwise velocity. However, it is well known that such spectra have a flat low-frequency region followed by a high-frequency roll off, so that locating the peak is difficult. Instead, one can look at the local pressure spectrum, which has a definite peak. Indeed, fig. 9 presents the PSD of pressure in the B118 jet at the same locations as in fig. 8(a). A monotonic decrease in the peak frequency is observed with increasing downstream distance.

This spectral analysis of pressure is carried out throughout the streamwise domain along the lipline for both the jets. The peak frequencies found thus are presented in fig. 10(a). The variation of St_{peak} with x/D_j is in the form of a rectangular hyperbola. Instead of fitting the data with a rectangular hyperbola directly, we found the average of the product of St_{peak} and x/D_j, presented in fig. 10(b). The result is

$$St_{peak} \approx \frac{2}{x/D_j}. \tag{15}$$

The new model for the frequency-dependent streamwise length scale l_x may now be constructed based on the foregoing. In particular, one would want to keep the variation with St unchanged from the existing model of eqn. (8). However, one should ensure its matching with the corresponding local frequency-independent scale ℓ_x at the local peak frequency that scales approximately as $2D_j/x$. The consequent new model is

$$l_x(\boldsymbol{x}, St) = \ell_x(\boldsymbol{x}) \frac{2D_j}{St\, x} \frac{1 - \exp\{-c_f St\}}{1 - \exp\{-2c_f D_j/x\}}. \tag{16}$$

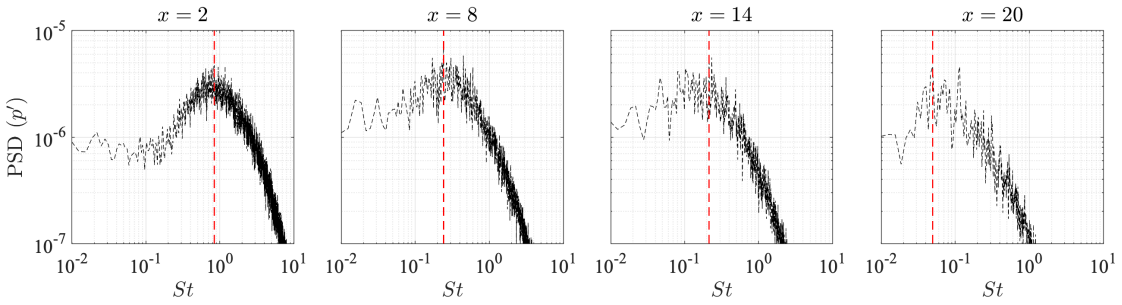

Fig. 9 **Power spectral density of pressure fluctuation at various streamwise locations along the lipline for the B118 jet. The red dashed lines indicate the respective peak locations, St_{peak}.**

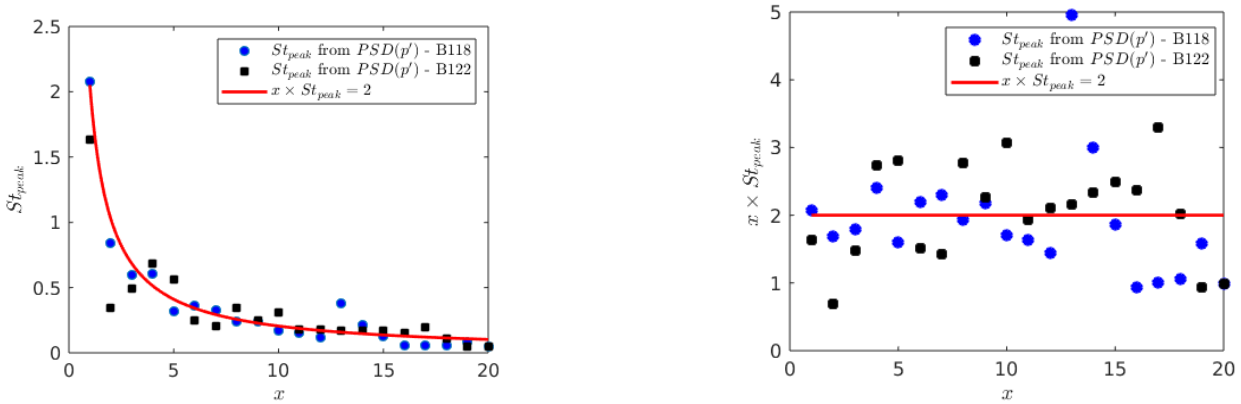

(a) (b)

Fig. 10 **Variation of (a) peak frequency St_{peak}, and (b) $x \times St_{peak}$, along the lipline in the streamwise direction, with implicit normalization of x with D_j.**

The length scales obtained using equation eqn. (16) are also plotted in fig. 8. The ℓ_x input to this comes from the correlation data. For both the jets, the proposed model matches very well with the results from the coherence data along the lipline throughout the entire streamwise domain studied. This model may fail to provide an accurate prediction of the frequency-dependent length scale very close to the jet exit. However, this is not concerning since the contribution of the noise sources from very near the jet exit is quite negligible.

The far-field spectra are recalculated with the proposed new model. Since the spectral shapes have changed from before, the amplitude constants are optimized again; we now have

$$B_0 = 0.026, \quad B_{>0} = 2.917. \tag{17}$$

Figure 11 presents the resulting predicted spectra at all the polar locations reported by Brès et al. [12], for both the jets. The predictions from the existing l_x model are also repeated from fig. 6 for the common polar angles, and filled in at the new ones. (The same line colour and marker style are retained from the earlier figure for continuity.) Overall, one may observe a continued good agreement with the reference FW-H spectra. Changes from the 'old' model results are minor, and are almost entirely concentrated at the higher end of the frequency spectrum at aft polar angles. Nonetheless, it must be recalled here that the amplitude constants had to be changed between the two models to obtain these matches.

IV. Conclusion

This paper investigates the source model used in an existing round jet noise prediction scheme based on steady RANS solution fields. The validity of the source model can only be evaluated by taking recourse to a higher-fidelity flow solution. For this purpose, extensive use is made of the well-validated LES database of Brès et al. [12] comprising of an isothermal and a heated Mach 1.5 jets, both expanded ideally.

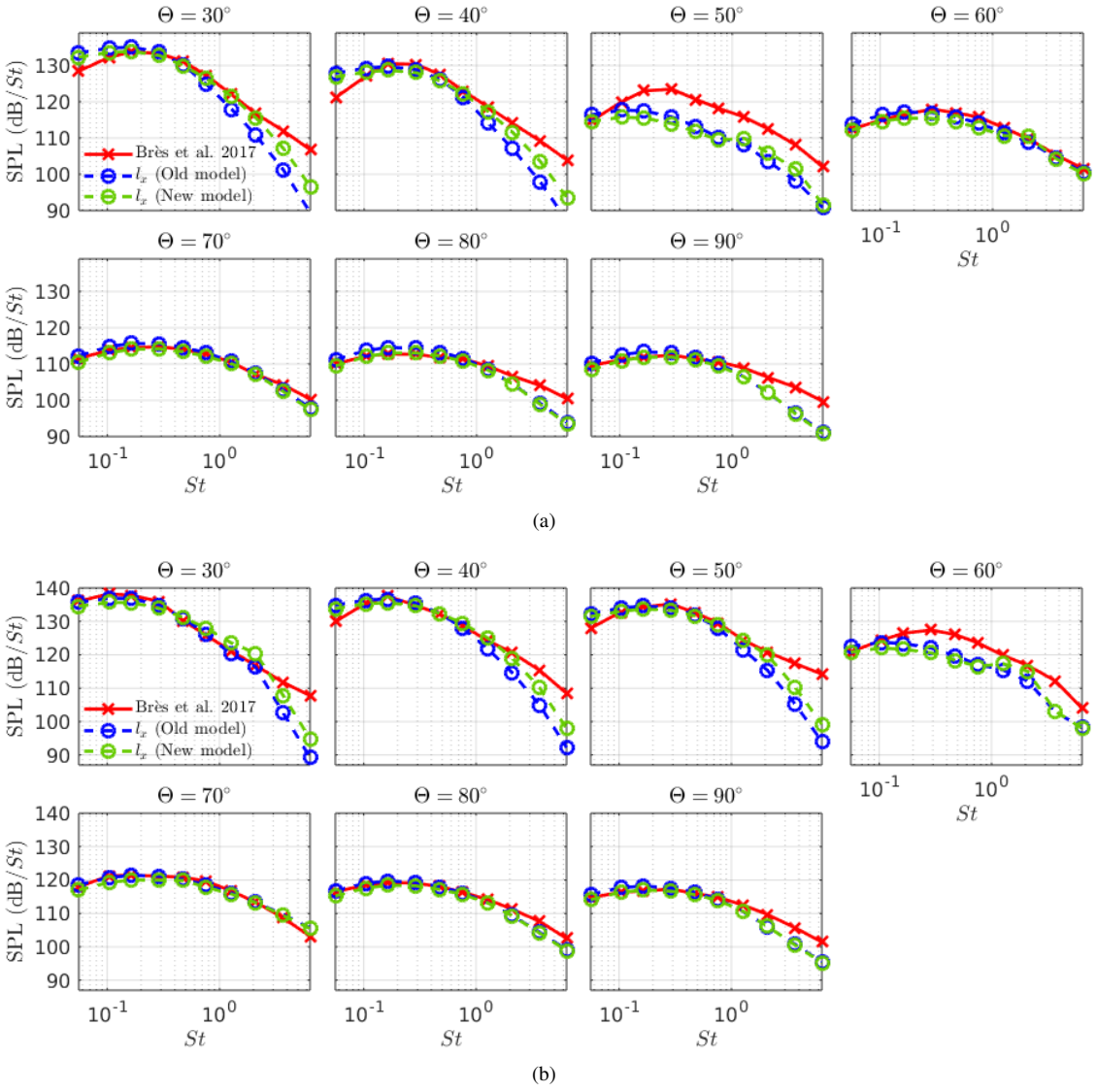

Fig. 11 **Comparison of the far-field noise predicted using the new frequency-dependent length scale model (l_x (New Model)) and existing frequency-dependent length scale model (l_x (Old Model)) for the (a) B118 and (b) B122 jets.**

In the noise source model, the turbulence in the jet flow is described by a model of the two-point two-time cross-correlation of the flow fluctuations, characterized by the turbulent length, time, and velocity scales. The local turbulent length and time scales are modelled using simple combinations of the local mean turbulent kinetic energy $\overline{K}$ and dissipation rate $\overline{\epsilon}$. These estimates of the length and time scales compare very well with those computed from the spatio-temporal cross-correlation of the streamwise velocity fluctuations in the LES jet database along the jets' lipline. The turbulent scales computed from the correlation data was used for the far-field noise prediction. The far-field sound predictions show very encouraging agreement with the Ffowcs Williams-Hawkings (FW-H) results that has a much higher input burden – viz. the time-resolved LES solution itself. In the process, we confirm the validity of the existing noise prediction model based on $\overline{K} - \overline{\epsilon}$ that may be obtained from a RANS simulation.

One of the ingredients of the above noise source model is a model of the local frequency-dependent length scale l based on the corresponding frequency-independent scale ℓ (the one described above). To probe this further, the cross-coherence was computed from the LES database, and it was fitted with a Gaussian decay function to find l. It was found that the existing model yields a very poor quantitative prediction of l, although the local qualitative trend with

frequency is well predicted. Based on extensive analysis, a new model is proposed for l that is in superior agreement with the results from the cross-coherence in the jet plume. The old l model was replaced in the overall noise source model with the new l model, and the far-field spectra were recalculated after re-optimizing the free amplitude parameters. Surprisingly, only a very slight improvement in the far-field spectra is obtained with the new model over the earlier one. The minor gains are limited to high frequencies at aft angles.

Given the significant improvement in the l predictions within the jet, these very modest improvements in the far-field sound estimates may be disheartening. However, it also points to the essential robustness of the RANS-based jet noise prediction approach studied here.

Acknowledgments

The authors are grateful to Dr. Guillaume Brès for sharing the LES solutions for the two supersonic jets, without which this work would not have been possible. Funding from a research grant from Indian Space Research Organization is also gratefully acknowledged.

References

[1] Tam, C. K. W., and Chen, P., "Turbulent mixing noise from supersonic jets," *AIAA Journal*, Vol. 32, No. 9, 1994, pp. 1774–1780.

[2] Lighthill, M. J., "On sound generated aerodynamically I. General theory," *Proceedings of the Royal Society of London A*, Vol. 211, No. 1107, 1952, pp. 564–587.

[3] Lilley, G. M., "On the noise from jets," Tech. Rep. CP-131, AGARD, 1974.

[4] Goldstein, M. E., "A generalized acoustic analogy," *Journal of Fluid Mechanics*, Vol. 488, 2003, pp. 315–333.

[5] Tam, C. K. W., and Auriault, L., "Jet mixing noise from fine-scale turbulence," *AIAA Journal*, Vol. 37, No. 2, 1999, pp. 145–153.

[6] Morris, P. J., and Farassat, F., "Acoustic analogy and alternative theories for jet noise prediction," *AIAA Journal*, Vol. 40, No. 4, 2002, pp. 671–680.

[7] Morris, P. J., and Boluriaan, S., "The prediction of jet noise from CFD data," *10th AIAA/CEAS Aeroacoustics Conference, paper 2977*, 2004.

[8] Raizada, N., and Morris, P. J., "Prediction of noise from high speed subsonic jets using an acoustic analogy," *12th AIAA/CEAS Aeroacoustics Conference, paper 2596*, 2006.

[9] Balsa, T. F., "The far field of high frequency convected singularities in sheared flows, with an application to jet-noise prediction," *Journal of Fluid Mechanics*, Vol. 74, No. 2, 1976, pp. 193–208.

[10] Goldstein, M. E., *Aeroacoustics*, McGraw-Hill Book Co.,New York, 1976.

[11] Miller, S. A. E., "Toward a comprehensive model of jet noise using an acoustic analogy," *AIAA Journal*, Vol. 52, No. 10, 2014, pp. 2143–2164.

[12] Brès, G. A., Ham, F. E., Nichols, J. W., and Lele, S. K., "Unstructured large-eddy simulations of supersonic jets," *AIAA Journal*, Vol. 55, No. 4, 2017, pp. 1164–1184.

[13] Tam, C. K. W., and Auriault, L., "Mean flow refraction effects on sound radiated from localized sources in a jet," *Journal of Fluid Mechanics*, Vol. 370, 1998, pp. 149–174.

[14] Ribner, H. S., "The generation of sound by turbulent jets," *Advances in Applied Mechanics*, Vol. 8, Elsevier, 1964, pp. 103–182.

[15] Morris, P. J., and Zaman, K. B. M. Q., "Velocity measurements in jets with application to noise source modeling," *Journal of Sound and Vibration*, Vol. 329, No. 4, 2010, pp. 394–414.

[16] Ffowcs Williams, J. E., and Hawkings, D. L., "Sound generation by turbulence and surfaces in arbitrary motion," *Philosophical Transactions of the Royal Society of London A*, Vol. 264, 1969, pp. 321–342.

[17] Schlinker, R., Simonich, J., Reba, R., Colonius, T., and Ladeinde, F., "Decomposition of high speed jet noise: Source characteristics and propagation effects," *14th AIAA/CEAS Aeroacoustics Conference, paper 2890*, 2008.

[18] Troutt, T. R., and McLaughlin, D. K., "Experiments on the flow and acoustic properties of a moderate-Reynolds-number supersonic jet," *Journal of Fluid Mechanics*, Vol. 116, 1982, pp. 123–156.

[19] Gudmundsson, K., "Instability wave models of turbulent jets from round and serrated nozzles," Ph.D. thesis, California Institute of Technology, 2010.

[20] Wang, G., Yang, F., Wu, K., Ma, Y., Peng, C., Liu, T., and Wang, L.-P., "Estimation of the dissipation rate of turbulent kinetic energy: A review," *Chemical Engineering Science*, Vol. 229, 2021, p. 116133.

[21] Sheng, J., Meng, H., and Fox, R., "A large eddy PIV method for turbulence dissipation rate estimation," *Chemical engineering science*, Vol. 55, No. 20, 2000, pp. 4423–4434.